# Tunneling spectroscopy of an indium adatom precisely manipulated on the cross-sectional surface of InAs/GaSb quantum structures

Kyoichi Suzuki,[1,2,*] Koji Onomitsu,[2] and Kiyoshi Kanisawa[2]

[1]*Fukuoka Institute of Technology, 3-30-1, Wajiro-Higashi, Higashi-ku, Fukuoka 811-0295, Japan*

[2]*NTT Basic Research Laboratories, NTT Corporation, 3-1 Morinosato-Wakamiya, Atshugi-shi, Kanagawa 243-0198, Japan*

(Received 11 October 2019; revised manuscript received 4 November 2019; published 18 December 2019)

Indium atom manipulation was achieved on the (110) cross-sectional surface of a quantum structure consisting of InAs/GaSb multilayer using a scanning tunneling microscope (STM) at low temperature. Positioning, removing, and lateral displacement by means of tip-induced hopping was performed on both InAs and GaSb layers. Electron tunneling via the electron orbital of the manipulated atom (adatom) was observed not only on the InAs layer but also on the GaSb layer, even when the energy of the orbital was in the GaSb band gap. The tunneling process from the STM tip to the InAs conduction band via the adatom and the GaSb band gap is explained well by the single electron tunneling model through the double-barrier tunneling junction. In the case of the adatom being very close to the InAs/GaSb heterointerface, interference with the electron tunneling to the InAs conduction electronic states through the GaSb barrier with/without passing the adatom was observed. The peak energy in the tunneling spectrum corresponding to the orbital of the adatom depends on the adatom position on the GaSb, demonstrating the fundamental interactions between the surface atomic-scale structures and semiconductor heterostructures.

DOI: 10.1103/PhysRevB.100.235306

## I. INTRODUCTION

To achieve the goal of semiconductor devices with high integration capability and low power consumption, atomic-scale devices are highly desirable. Progress in atom manipulation techniques is therefore urgently required. Scanning probe microscopes (SPMs) are a promising tool for constructing these devices. SPM atom manipulation is widely used in/on metal surfaces [1–3]; it has also recently been used in/on semiconductor surfaces [4–9]. In particular, among the existing SPMs, the scanning tunneling microscope (STM) is a powerful tool because it can be used not only for atom manipulation but also for spectroscopy of the quantum structures composed of the manipulated atoms [7–9].

So far, SPM atom manipulation has been performed on/in homogeneous surfaces because a flat and clean surface is essential. As one step further, we have investigated SPM atom manipulation on artificial quantum structures. New functionalities are expected from the wave-function coupling between the constructed atomic-scale structures and the template with quantum structures.

In this paper, we report In atom manipulation on a cross-sectional surface of InAs/GaSb multilayers using a low-temperature STM. Atom manipulation was successively achieved on both InAs and GaSb layers. In addition, electron tunneling via the orbital of the manipulated atom (adatom) was investigated. In particular, not only on the InAs layer but also on the GaSb layer, electron tunneling via the adatom has been detected. This was in spite of the energy of the orbital being in the GaSb band gap. To explain this tunneling process, we adopt the single electron tunneling model through the double-barrier tunneling junction. By selecting suitable parameters in the equivalent circuit, the tunneling properties are reproduced well. In addition, we discuss the orbital energy of the adatom in terms of the distance between the adatom on the GaSb layer and the heterointerface.

## II. EXPERIMENTAL PROCEDURES

As a template for the atom manipulation, an InAs(16 nm)/GaSb(16 nm) multilayer structure was grown by molecular beam epitaxy on a 400-$\mu$m-thick conductive InAs(001) substrate. To obtain a clean and flat (110) cross-sectional surface, the template was loaded into an ultrahigh-vacuum (UHV) chamber at $10^{-10}$ Torr and cleaved with tweezers. Following this, the template was transferred to the STM setup, which was cooled to 4.8 K without breaking the UHV condition. Electrochemically etched tungsten wire was used as the STM tip. Bias voltage is applied to the template relative to the tip (set neutral). The experimental setup and preparation are the same as those in Refs. [8,10]. A wide and flat template with an area of more than 10 $\mu$m$^2$ can be easily obtained without any atomic steps. In contrast with the epitaxial surface, i.e., the InAs (111)A surface [7,9], there are no native adatoms on the cleaved (110) surface of the InAs bulk crystal or InAs/GaSb heterostructures.

During the *in situ* STM tip preparation by applying a voltage pulse between the tip and the InAs substrate in the template or by bringing it into contact with the substrate far away from the quantum structures, many In atoms stick to the tip. Therefore, we can start to transfer In atoms one-by-one from the tip to the surface notwithstanding the absence of native adatoms on the cleaved surface. After the repeated atom

*k-suzuki@fit.ac.jp

 

positioning processes, there comes a juncture where no atom can be transferred from the tip to the surface. This can be attributed to the lack of the atoms on the tip. In this situation, after touching the tip with the InAs surface, the atom can be transferred from the tip and positioned on the GaSb or InAs surface again. In contrast, after touching the tip with the GaSb surface, even when we try to position the atom on a different place, no atom can be transferred from the tip. In addition, the transferred atom is always positively charged and shows the characteristics of the In atom [11], as exhibited later. Therefore, we conclude that the transferable and manipulatable atom is In, not Ga, Sb, or As.

For scanning tunneling spectroscopy (STS), the scanning area of the topographic image is divided pixel-wise. After the STM tip is fixed at a tunneling current $I$ and a sample bias voltage $V$, the differential tunneling conductance $(dI/dV)$ and $I$ are measured simultaneously per pixel with sweeping $V$ using a lock-in amplifier with a small voltage modulation of 20 $mV_{pp}$, 700 Hz. Here, the normalized differential conductance $[(dI/dV)/(I/V)]$ corresponds to local density of states (LDOS) as a function of the energy $(eV)$ from the Fermi level, where $e(>0)$ is the elementary charge. In contrast, for simple tunneling spectroscopy at a point, on an adatom for example, $I$ is measured ten times with sweeping $V$ at fixed tip height and then averaged. LDOS is numerically obtained from averaged $I$ by differentiation and normalization. This is because the noise in the $(dI/dV)$ signal from the lock-in amplifier is relatively large, in particular for the adtom on GaSb, due to the small tunneling current and its small change as a function of $V$. In both cases, for avoiding the divergence of LDOS due to division by nearly zero at low voltage region, a small constant is added to the denominator $(I/V)$. Although this method is generally applied, the LDOS spectra discussed later include unavoidable unintentional broadening [12]. In particular, for LDOS measured on the adatoms, we took care not to change the LDOS spectra shape during this process.

## III. RESULTS AND DISCUSSION

### A. Cross-sectional STM/STS images

Figure 1(a) shows an STM image of the cross-sectional surface of the template with four manipulated adatoms on the central InAs layer, where there is no atomic step. The contrast between the layers depends on the electronic structure of each material. With positive sample voltage $V = +1.0$ V, the InAs layer appears brighter than the GaSb layer. In contrast, with negative sample voltage $V = -1.0$ V, the GaSb layer appears brighter than the InAs layer. The schematic energy band profile of the template is shown in Fig. 1(b). In this InAs/GaSb heterostructure system, the conduction band bottom of InAs is 0.15 eV lower than the valence band top of GaSb. Without intentional doping, the Fermi level lies in the band overlap region [13]. As a result, all layers are conductive and suitable for STM measurements. The InAs layer becomes a quantum well (QW) for the conduction band and the GaSb layer becomes a QW for the valence band. Electron and hole wave functions are confined in each QW and quantized subbands are formed [14,15]. The available position of the adatom is described as a stick-and-ball model for the surface

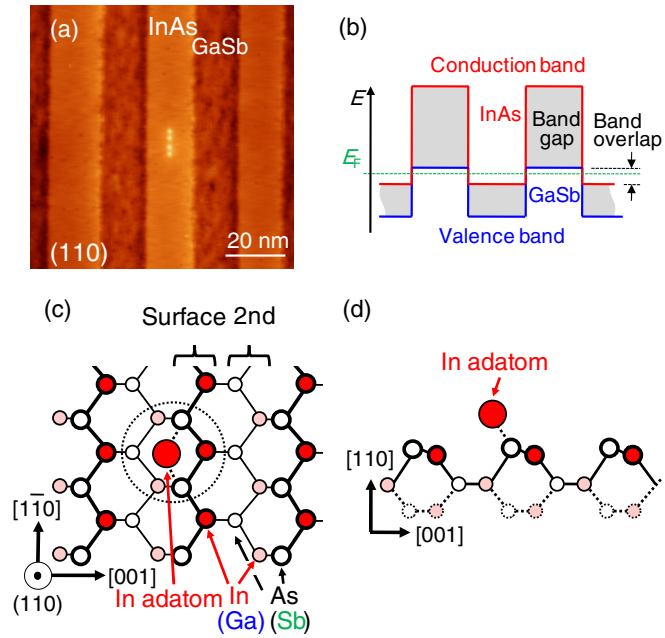


FIG. 1. (a) STM image of (110) cross-sectional surface of InAs(16 nm)/GaSb(16 nm) quantum structures with four manipulated adatoms on an InAs layer (sample bias voltage $V = +1.0$ V and feedback tunneling current $I = 200$ pA). (b) Schematic energy band profile for InAs/GaSb quantum structures. (c) Stick-and-ball model for the (110)InAs (GaSb) surface with one manipulated adatom and (d) its cross section.

and cross section in Figs. 1(c) and 1(d), respectively. On the (110) surface of InAs (GaSb), zigzag chains composed of In (Ga) and As (Sb) atoms are regularly aligned on the surface. The positioned adatom is adsorbed by weak ionic bonds to the adjacent anionic As (Sb) atoms on the surface.

As evidence of the quantum structures formed in the template, the spatial mapping of LDOS in an InAs electron QW obtained by STS is shown in Fig. 2. Figure 2(a) shows the STM image of the InAs QW. The central bright region is the InAs QW layer and the dark regions on both sides are the GaSb barrier layers. The LDOS maps at different energies are shown in Figs. 2(b)–2(f). Bright regions indicate a high LDOS. The LDOS maps clearly show the formation of quantized electron subbands confined in the QW. At $V = 0.15$ V, only one vertical fringe appears in the QW center as a squared wave function of the ground (first) subband [Fig. 2(b)]. With increasing $V$, the number of fringes increases, corresponding to an increase in the subband indices [Figs. 2(c)–2(f)]. These brighter fringes correspond to the sum of the LDOS for the subbands existing at the energy $eV$ because each subband has degrees of freedom parallel to the layer [14]. For the explanation, the schematic diagram of the total LDOS is shown in Fig. 2(g). These curves correspond to the total LDOS from the ground to the highest subband at an energy. For example, the curve arrowed in the upper side corresponds to the total LDOS from the ground to sixth subbands. As shown in Figs. 2(f) and 2(g), with increasing the subband indices, the total LDOS tend to distribute to the heterointerface on both sides. Furthermore, it is expected that more LDOS penetrate the GaSb barriers. This penetration is important for the discussion in Sec. III C.

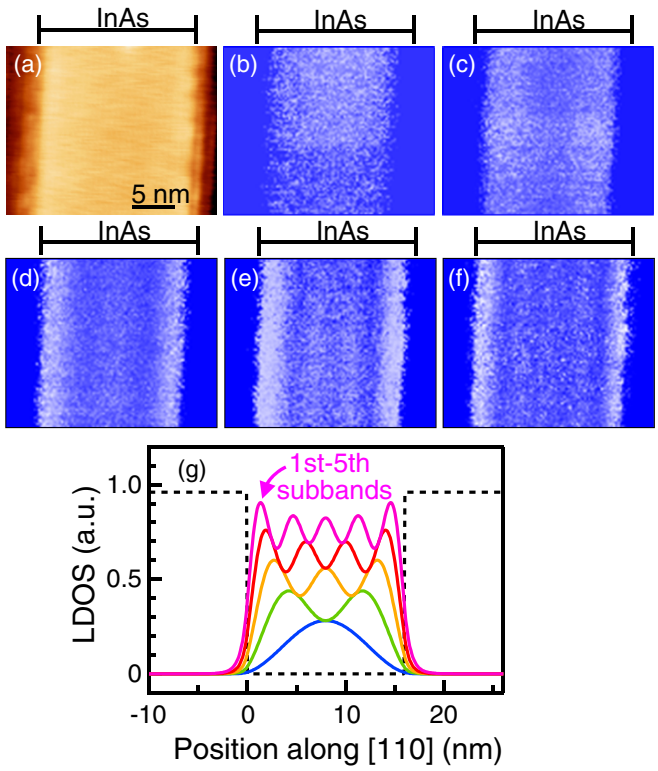


FIG. 2. (a) STM image focusing on an InAs electron QW ($V = 1.0$ V, $I = 200$ pA). (b)–(f) LDOS maps obtained at $V = 0.15$, 0.25, 0.5, 0.625, and 0.825 V, respectively. (g) Schematic diagram of the spatial distribution of LDOS. The position between 0 and 16 nm corresponds to the InAs QW. Each curve corresponds to the sum of LDOS (squared wave functions) for subbands. For example, the arrowed curve is the sum of the LDOS from first (ground) to fifth subbands. The dotted line indicates the conduction band offset in energy (eV) composed of 0.81 eV for the GaSb band gap and 0.15 eV for the band overlap between the InAs conduction and GaSb valence bands.

In contrast, in the case of the GaSb hole QW for this template, the subband formation cannot be identified (not shown) because many subbands are generated in a small energy region due to the large effective mass of holes ($m_{\mathrm{eff}} = 0.36m_0$, where $m_0$ is the static electron mass). For example, the energy separation between the ground and second subbands is expected to be only 4 meV, which is much smaller than the sample voltage modulation for STS measurements. When we perform STS on a thinner GaSb QW structure, the subband formation of holes can be clearly identified [15].

### B. Atom manipulation and tunneling spectroscopy

The atom manipulation procedure is similar to those used for the homogeneous InAs(111)A and (110) surfaces [7–9]. For the positioning process, the STM tip approaches the surface with negative $V$. In contrast, for the removal process, the tip approaches with positive $V$. In addition, by sweeping $V$ on the target adatom, it can be excited to hop along the [001] direction (not the [00$\bar{1}$] direction) by one atomic row. The direction is determined by the inversion asymmetry on the surface along [001] shown in Figs. 1(c) and 1(d). Due

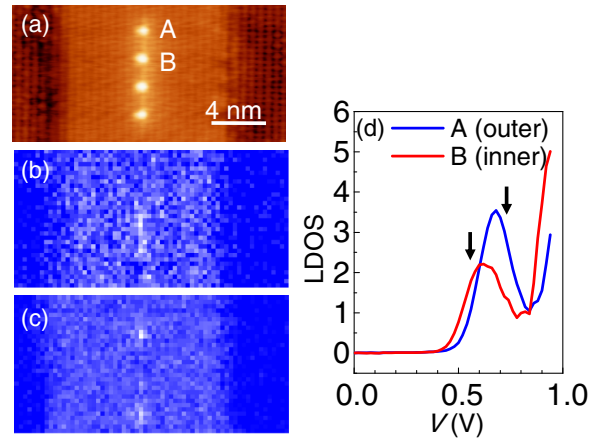


FIG. 3. (a) STM image of four assembled In adatoms on an InAs QW ($V = 1.0$ V, $I = 200$ pA). The distance between the adjacent adatoms is $\frac{5}{\sqrt{2}}a$, where $a = 0.606$ nm is the lattice constant. (b) and (c) LDOS maps over the area in (a) at $V = 0.57$ and 0.73 V [corresponding to the arrows in (d)], respectively. (d) LDOS spectra as a function of $V$ measured on adatoms "A" and "B" in (a).

to the inelastic tunneling excitation, the atom is vibrationally excited. Once the atom exceeds the nearest potential hills, which consist of cationic In atoms in the zigzag row on the right-hand side [Fig. 1(c)], the adatom never returns to its initial position. As a result, it hops by one atomic row in the [001] direction without hopping along the [1$\bar{1}$0] or [$\bar{1}$10] direction [8].

The electronic structures of the assembled adatom chain are shown in Fig. 3(a). Four adatoms are vertically aligned on an InAs layer with a constant distance of $\frac{5}{\sqrt{2}}a$ between them, where $a = 0.606$ nm is the lattice constant. The LDOS spectra obtained on the outer adatom (A) and inner adatom (B) are shown in Fig. 3(d). In addition, spatial distributions of the LDOS are mapped at different sample voltages in Figs. 3(b) and 3(c), which correspond to the arrows in Fig. 3(d). The observed LDOS (bright regions) correspond to the 5$p$-like orbital of the In adatoms [11]. At $V = 0.57$ V (lower energy), the LDOS mainly accumulates on the inner two adatoms. In contrast, at $V = 0.73$ V (higher energy), it mainly accumulates on the outer atoms. Clear moleculelike coupling of the manipulated adatoms has been observed in the InAs QW. Although faint fringes corresponding to the QW subbands were observed in the background, clear evidence of the interaction between the moleculelike coupled adatoms and subband structures in the template was not identified clearly. This might be due to difficulty in the closer tip approach. To detect the LDOS change in the QW with high sensitivity, the tip-sample distance should be as short as possible. However, a very short tip-sample distance causes unintentional adatom hopping in the case of the (110) surface. Therefore, we must maintain a relatively long tip-sample distance, which degrades the sensitivity during LDOS measurements.

On the GaSb layer, the In atom manipulation processes (positioning, removing, and hopping along the [001] direction) were also found to be available in the same manner as above. However, the adatom is rather unstable compared to the InAs layer (discussed later). When the tip-sample distance is

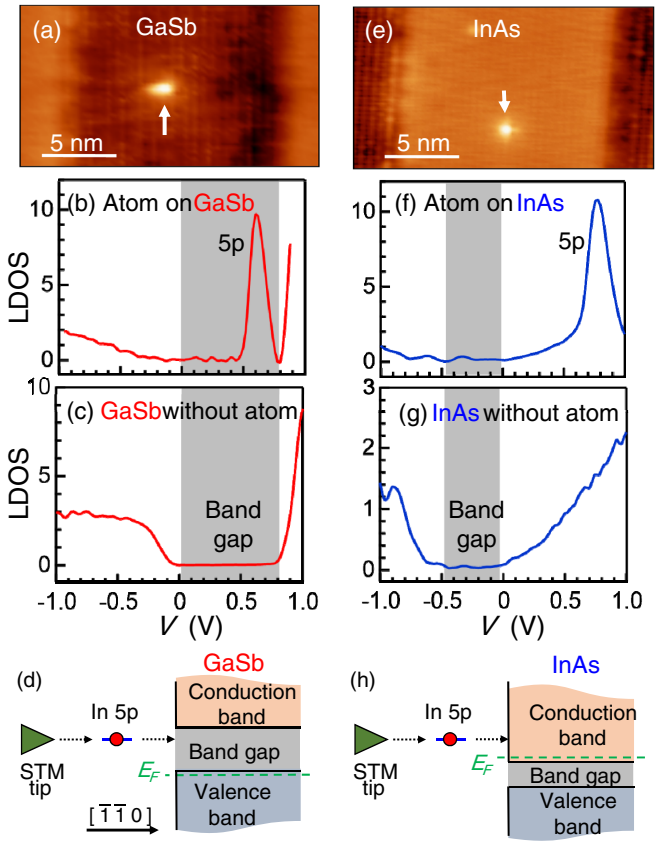


FIG. 4. (a) STM image of one adatom positioned at the center of a GaSb layer ($V = 1.0$ V, $I = 100$ pA). (b) and (c) Tunneling spectra measured on the adatom and on the GaSb layer without an adatom. (d) Schematic energy diagram of the tunneling process on the GaSb layer via the positioned adatom. For clarity, the potential modulation due to the positively charged adatom discussed in a later part is not shown. (e)–(h) Corresponding panels for an InAs layer.

short at positive sample voltage, at $I = 200$ pA and $V = 1.0$ V for example, the adatom unintentionally hops along the [001] direction with every scan. Finally, the adatom settles at the interface between the GaSb and InAs layers. An STM image of a manipulated adatom on the GaSb layer observed at $I = 100$ pA and $V = 1.0$ V is shown in Fig. 4(a). In this condition, the adatom rather stably stays on the GaSb layer. The adatom is visible as a bright spot, indicating that the tunneling current flows via the adatom. Comparing with the adatom on the InAs layer, shown in Fig. 4(e), the adatom on the GaSb layer appears elongated along the scanning direction. This suggests that the adatom slightly shifts and moves back during the scan because the tip is biased 1.0 V negative at the positive $V$ applied to the template. Then, the tip attracts the adatom, which is positively charged.

LDOS spectra measured on this adatom and on the GaSb layer without an adatom are plotted in Figs. 4(b) and 4(c), respectively. For comparison, the corresponding LDOS spectra for the InAs layer are shown in Figs. 4(f) and 4(g). As mentioned above, the peaks observed in Figs. 4(b) and 4(f) originate from the $5p$-like orbital of the adatom. The low LDOS (gray) regions in Figs. 4(c) and 4(g) correspond to the band gaps of the GaSb and InAs, respectively. In the case of InAs, the band gap including the quantum confinement ranges approximately from $-0.5$ to 0 V. The positive voltage region in Fig. 4(g) corresponds to the conduction band of the InAs. Then, the LDOS peak of the $5p$-like orbital is in the InAs conduction band. It is natural that the electrons injected from the tip tunnel via the $5p$-like orbital states, which are in resonance with the states in the conduction band, as shown in Fig. 4(h). The LDOS peak width (full width at half maximum) is 0.22 eV for the adatom on InAs, which is wider than that for the adatom on GaSb (0.16 eV). This also indicates that the $5p$-like orbital states of the adatom on InAs are in resonance with the conduction band. In contrast, the GaSb band gap ranges approximately from 0 to 0.8 V. The LDOS peak of the $5p$-like orbital is found in the band gap of the GaSb. Here, the question arises as to where the electrons tunnel via the manipulated adatom, as shown in Fig. 4(d).

### C. Tunneling via the adatom on the GaSb layer

Thus far, electron tunneling via the adatom on an InAs bulk crystal has been studied [8]. This tunneling process was found to be fundamentally similar to that on the InAs layer in the InAs/GaSb heterostructure as mentioned above. In this section, we focus on electron tunneling via the adatom on the GaSb layer. To further elucidate the tunneling process, we measured the LDOS spectra for the adatoms at different positions on the GaSb layer.

Representative STM images are shown in Figs. 5(a)–5(d), and the corresponding LDOS spectra measured on these adatoms are plotted in Figs. 5(e)–5(h), respectively. Here, the adatom position was changed by atom manipulation as described above. To avoid unintentional adatom hopping, the feedback tunneling current was lowered to $I = 50$ pA at $V = 1.0$ V before sweeping $V$. This implies that the tip adatom distance during the LDOS measurement was longer than that in Fig. 4(a). The voltage was swept from 0 to 0.9 V except for the case in Fig. 5(h) (from 0 to 1.0 V). The peak position of $V$ is slightly lower than that in Fig. 4(b). The shapes of the spectra are almost identical for Figs. 5(e)–5(g). In contrast, the shape is significantly different in Fig. 5(h), where a long tail is observed on the lower voltage side of the peak, although the change in the adatom position between Fig. 5(c) and 5(d) is only 1.2 nm. On the high voltage side of the peak ($V > 0.8$ V), LDOS increases as a function of $V$ due to the direct tunneling to the GaSb conduction band from the tip.

In Figs. 6(a) and 6(b), the LDOS peak voltage and width in $V$ are plotted as a function of the adatom position. The gray regions correspond to the InAs layers on both sides. The positions zero and 16 nm correspond to the InAs/GaSb heterointerfaces. Here, the peak width is determined by double the half width at half maximum on the high-voltage side of the Gaussian fitted peak because the peak shapes are asymmetric. Arrows correspond to Figs. 5(e)–5(h) from left to right. The peak voltage slightly depends on the adatom position on the GaSb layer. The peak voltage tends to increase as the adatom approaches the heterointerface. The peak width is almost independent of the adatom position except when the adatom is nearest to the heterointerface [Fig. 5(h)].

Thus far, single electron transport of a single donor atom has been investigated for application to new types of Si

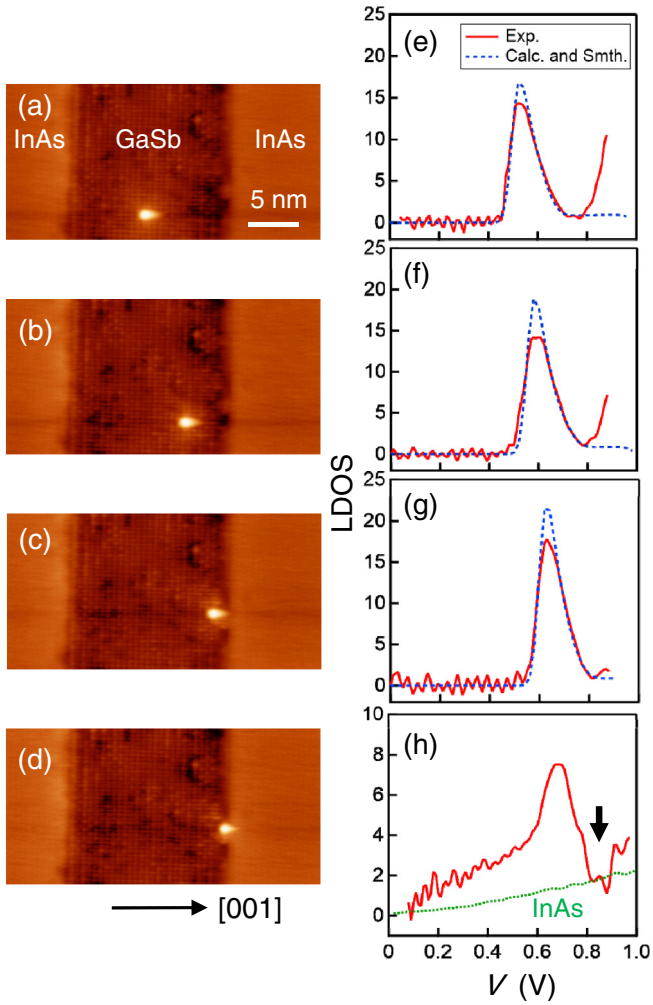


FIG. 5. (a)–(d) STM images of one adatom on a GaSb layer at different adatom positions ($V = 1.0$ V, $I = 50$ pA). (e)–(h) Corresponding tunneling spectra measured on the adatom (red solid line) and reproduced tunneling spectra using a single electron tunneling model with double-barrier tunneling junction (blue dashed line). The green dotted line in (h) is the spectrum obtained on the InAs layer without adatom [same as Fig. 4(g)] for the sake of clarity. The arrow indicates the dip suggesting Fano resonance.

field effect transistors [16,17]. Electron tunneling between the donor and source or between the donor and drain of more than 100 nm in length was observed. On the basis of these results, it is natural to consider electron tunneling between the $5p$-like orbital of the adatom and the InAs conduction band in our case. Schematic diagrams are depicted in Figs. 7(a) and 7(b). The adatom on the GaSb layer is positively charged, like an ionized donor impurity. Therefore, the potential barrier, i.e., the energy bands of the GaSb, is strongly modulated. The effective barrier height is lowered and tunneling becomes possible. As a result, a double-barrier tunneling junction (DBTJ) between the tip and adatom, and between the adatom and adjacent InAs layers are formed.

The adatom gains charging energy by electron injection from the tip. Consequently, the next electron injection is hindered while the electron remains in the adatom. The electron residence time ($\tau_r$) at the adatom estimated from the peak

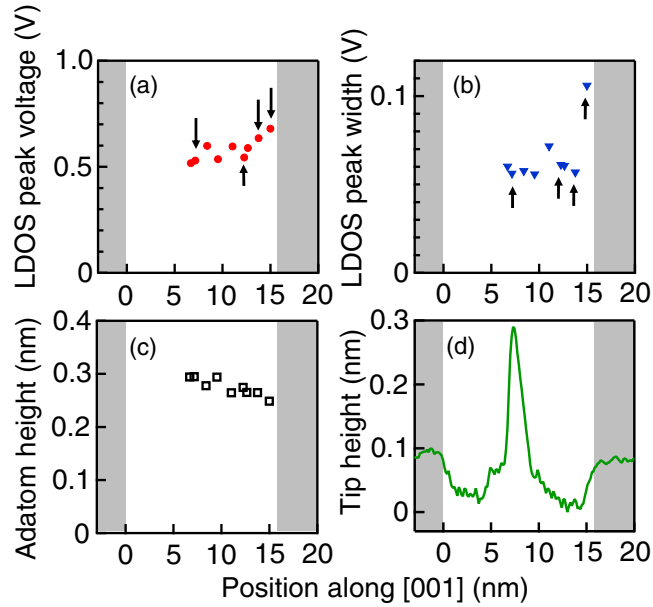


FIG. 6. (a) LDOS peak position and (b) width as a function of the adatom position from the heterointerface on the left-hand side. Gray regions correspond to the InAs layer. Arrows correspond to the spectra in Figs. 5(e)–5(h) from the left-hand side, respectively. (c) STM tip height measured on the adatom as a function of the adatom position. The lowest tip height in the topographic curve along [001] is set to zero. (d) Typical topographic curve as a function of position along [001], corresponding to the horizontal cross section on the adatom in Fig. 5(a).

width [Fig. 6(b)] is of the order of $10^{-14}$ s. In contrast, the average electron tunneling period ($\tau_i$) estimated from the tunneling current ($I = 50$ pA) is of the order of $10^{-8}$ s. $\tau_r \ll \tau_i$ is satisfied. This is similar to single electron tunneling via a quantum dot or single electron transistor. In general, such single electron transport through a DBTJ is calculated using the "orthodox" theory [18–21]. With reference to reports concerning electron transport via a nanoparticle on a thin insulating film with STM [19,20], we calculated the LDOS spectra.

The equivalent circuit is shown in Fig. 7(c). $C_1$ and $R_1$ represent the capacitance and resistance between the tip and adatom, respectively. $C_2$ and $R_2$ correspond to those between the adatom and InAs layers, respectively. In addition, the fractional residual charge $Q_0$ in the $5p$-like orbital is introduced. In the case of the quantum dots, $Q_0$ corresponds to the residual charge in the dot controllable by the gate. In contrast, in our case, although $Q_0$ is only the parameter, we consider it as the electron stay time in the $5p$ state through tunneling. Using these values as variable parameters, the tunneling current $I$ was first calculated as a function of $V$. Then the calculated $I$-$V$ data were averaged between $\pm 20$ mV to include the influence of the bias voltage modulation. Finally, the LDOS spectra were calculated by differentiation and normalization.

The calculated LDOS spectra are plotted as blue dashed lines in Figs. 5(e)–5(g). The employed parameters are plotted in Figs. 7(d)–7(f) [22]. The experimentally obtained LDOS spectra are well reproduced by the calculation in the case of the adatom in the middle of the GaSb layer. The fitting

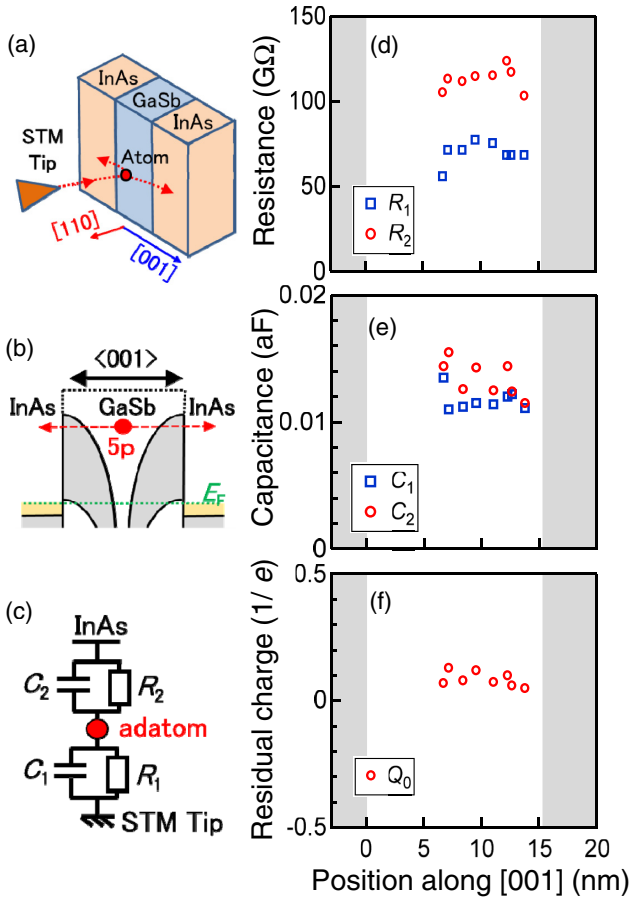


FIG. 7. (a) Schematic diagram of electron tunneling from the STM tip via the adatom on the GaSb layer to the InAs layers on both sides. (b) Schematic diagram of the modulated energy band with the positively charged adatom on the GaSb layer. The gray regions correspond to the band gap for each material. The black, dotted, rectangular line indicates the GaSb conduction band without a charged adatom. The red dashed arrows indicate the electron tunneling from the $5p$-like orbital of the adatom to the InAs layers. (c) Equivalent circuit model for the tunneling process. (d)—(f) Fitted parameters [(d) $R_1$ and $R_2$, (e) $C_1$ and $C_2$, (f) $Q_0$] as a function of the adatom position except for the adatom nearest the heterointerface [Fig. 5(d)].

parameters are mostly identical and insensitive to the adatom position. This could be attributable to the injected electrons being able to tunnel to the InAs layers on both sides. These calculation results also explain the asymmetric shape of the peaks. The rising point of $I$ with increasing $V$ corresponds to the starting point of the tunneling from the tip to the $5p$-like orbital, and also corresponds to the end of the Coulomb blockade region in the case of the quantum dot. Under the condition of an extremely low temperature, the $I$-$V$ curve would be expected to be disconnected at this point [18]. Even at a realistic low temperature, $I$ suddenly starts to increase at the point. As a result, the low-energy side of the LDOS peak becomes steep and the LDOS peak becomes asymmetric.

In contrast, the LDOS spectrum for the adatom nearest to the heterointerface [Fig. 5(h)] cannot be explained only by this single electron transport model with DBTJ. The LDOS spectrum in the experiment showed an increase from approximately 0 V and peaked at approximately 0.6 V. At least two electronic states would be necessary to explain this spectrum shape under this model [23]. If the system were a common quantum dot, which would have several discrete electronic states with constant energy gaps, it would be possible to reproduce this LDOS spectrum shape. The peak position (0.6 V in this case) would correspond to the resonant tunneling from the source to one state in the dot. The LDOS start point (approximately 0 V) would correspond to the resonant tunneling from the lower energy state to the drain. At that time, the residual charge $Q_0 \sim e/2$ would be assumed. However, in our case, it is different from the quantum dot. There is only one state, i.e., the $5p$-like orbital of the adatom. Another tunneling process must be considered in addition to the single electron transport with DBTJ, as discussed below.

In the case of the adatom on the InAs layer [Fig. 4(f)], the LDOS spectrum also begins increasing from 0 V, corresponding to the conduction band bottom of the InAs. The LDOS peak width is greater than that for the adatom on the GaSb layer because of resonance states formed between the $5p$-like orbital and the InAs conduction band. Even then, the component of the LDOS in the low-$V$ region is attributed to the tunneling between the tip and the InAs conduction band without passing the resonance states rather than the tunneling through spread resonance states. In the case of the adatom on the GaSb layer nearest to the heterointerface, the wave functions of the InAs conduction band have penetrated the GaSb layer, shown in Fig. 2(e). In the same manner, the component of the LDOS on the lower voltage side of the $5p$-like orbital [Fig. 5(h)] is attributed to the tunneling from the tip to the electron wave functions of the InAs conduction electronic states that have penetrated the GaSb layer without passing the $5p$-like orbital. For clarity, the LDOS spectrum obtained on the InAs layer without the adatom [same as Fig. 4(g)] is shown as the green dotted line.

Compared to the LDOS peak in Figs. 5(e)–5(g), the peak shown in Fig. 5(h) tails to the lower $V$ side and there is a notch structure on the higher $V$ side of the peak [arrow in Fig. 5(h)]. Although further investigation is necessary, the strong asymmetric line shape measured at the interface boundary signifies that there occurs a quantum mechanical interference phenomenon such as Fano resonance [24,25], resulting from the interference between the electron tunneling with and without passing the $5p$-like orbital of the adatom. Provided this interpretation consistently explains the experimental results, the tailing of the atomic resonance peak to the lower-energy side and the notch shape (antiresonance) at the higher-energy side reveal that the Fano asymmetry parameter is negative. This speculation describes that the majority effect is backscattering of the wave function due to inelastic tunneling, possibly through strong coupling with the adatom vibration.

### D. Quantum structure effect on adatom

In addition to the tunneling process, we investigated the relationship between the adatom height and $5p$-like orbital energy of the adatom on the GaSb. Figure 6(c) shows the STM tip height measured on the adatom at different adatom positions. The lowest tip height in the topographic curve

on the adatom along [001] is set to zero. For example, a typical topographic curve measured on the adatom is shown in Fig. 6(d), corresponding to the horizontal cross section of Fig. 5(a). Comparing Figs. 6(a) and 6(c), where the adatom position changes to the heterointerface, the adatom height decreases and $5p$-like orbital (LDOS peak) energy increases. These three, height, energy, and position, from the interface correlate to each other. This might come from the interaction between the adatom and electronic states in the InAs layer. Two candidate interactions are considered. One is electrostatic attraction between the positively charged adatom and electrons below the Fermi level in the InAs layer. The other is covalent bondlike quantum coupling between the $5p$-like orbital and empty states in the InAs layer. These interactions depend on the distance between the adatom and the InAs layer. Although further investigation is necessary to clarify how adatom height is affected by these interactions, the observed position dependence precisely indicates the degree and a tendency of the interaction between the manipulated atom and the heterostructure system.

## IV. CONCLUSION

We have achieved single In atom manipulation on the cross-sectional surface of the InAs/GaSb quantum structure. Positioning, removing, and sliding in a specific direction by one atomic row were successful on both InAs and GaSb layers, which are electron and hole QWs, respectively. In particular, on the GaSb layer, electron tunneling was observed via the atom in the GaSb band gap. We propose the tunneling process between the $5p$-like orbital of the atom and the InAs conduction band exceeding the GaSb barriers. Using the single electron tunneling model through the double-barrier tunneling junction, the LDOS spectra for the adatom on the GaSb layer around the middle are well reproduced. In contrast, in the case of the adatom on the GaSb nearest the heterointerface, another component was observed in the LDOS spectrum on the lower-energy side of the $5p$-like orbital. We attributed this component to the tunneling between the tip and InAs conduction electronic states penetrated into the GaSb layer without passing the $5p$-like orbital. In addition, we observed that the $5p$-like orbital energy of the adatom on the GaSb depends on the adatom height. This work serves as a basis for further fundamental studies of artificial atomic-scale structures fabricated with semiconductor heterostructures to develop novel next-generation quantum devices.

## ACKNOWLEDGMENT

We thank S. Sasaki for insightful discussions.

[1] D. M. Eigler and E. K. Schweizer, Nature (London) **344**, 524 (1990).
[2] J. A. Stroscio and D. M. Eigler, Science **254**, 1319 (1991).
[3] M. F. Crommie, C. P. Lutz, and D. M. Eigler, Science **262**, 218 (1993).
[4] I.-W. Lyo and Ph. Avouris, Science **253**, 173 (1991).
[5] G. Dujardin, A. Mayne, O. Robert, F. Rose, C. Joachim, and H. Tang, Phys. Rev. Lett. **80**, 3085 (1998).
[6] Y. Sugimoto, P. Pou, O. Custance, P. Jelinek, M. Abe, R. Perez, and S. Morita, Science **322**, 413 (2008).
[7] S. Fölsch, J. Yang, Ch. Nacci, and K. Kanisawa, Phys. Rev. Lett. **103**, 096104 (2009).
[8] K. Suzuki, S. Fölsch, and K. Kanisawa, Appl. Phys. Express **4**, 085002 (2011).
[9] V. D. Pham, K. Kanisawa, and S. Fölsch, Phys. Rev. Lett. **123**, 066801 (2019).
[10] K. Suzuki, K. Kanisawa, S. Perraud, M. Ueki, K. Takashina, and Y. Hirayama, J. Appl. Phys. **101**, 081705 (2007).
[11] K. Kanisawa, J. Cryst. Growth **378**, 8 (2013).
[12] R. M. Feenstra, J. Y. Lee, M. H. Kang, G. Meyer, and K. H. Rieder, Phys. Rev. B. **73**, 035310 (2006).
[13] K. Suzuki, K. Takashina, S. Miyashita, and Y. Hirayama, Phys. Rev. Lett. **93**, 016803 (2004).
[14] K. Suzuki, K. Kanisawa, C. Janer, S. Perraud, K. Takashina, T. Fujisawa, and Y. Hirayama, Phys. Rev. Lett. **98**, 136802 (2007).
[15] K. Suzuki, K. Kanisawa, S. Perraud, and T. Fujisawa, Appl. Surf. Sci. **254**, 7889 (2009).
[16] H. Sellier, G. P. Lansbergen, J. Caro, S. Rogge, N. Collaert, I. Ferain, M. Jurczak, and S. Biesemans, Phys. Rev. Lett. **97**, 206805 (2006).
[17] E. Hamid, D. Moraru, Y. Kuzuya, T. Mizuno, L. T. Anh, H. Mizuta, and M. Tabe, Phys. Rev. B **87**, 085420 (2013), and references therein.
[18] A. E. Hanna and M. Tinkham, Phys. Rev. B **44**, 5919 (1991).
[19] D. Porath, Y. Levi, M. Tarabiah, and O. Millo, Phys. Rev. B. **56**, 9829 (1997).
[20] H. Zhang, Y. Yasutake, Y. Shichibu, T. Teranishi, and Y. Majima, Phys. Rev. B **72**, 205441 (2005).
[21] R. Nuryadi, Master equation-based numerical simulation in a single electron transistor using Matlab, in *Numerical Simulations of Physical and Engineering Processes*, edited by J. Awrejcewicz (InTech, Rijeka, Croatia, 2011).
[22] The tip height is fixed at $I = 50$ pA and $V = 1.0$ V. This corresponds to 20 GΩ. However, the energy (1.0 eV from the Fermi level) is higher than the GaSb conduction band bottom. Therefore, the tunneling to the GaSb conduction band from the tip is dominant. On the lower-energy side, the current is composed of only the tunneling via the adatom. As a result, the resistance becomes much higher. The fitting has been conducted between $V = 0$ and 0.9 V. The resistance between 50 and 100 GΩ is reasonable.
[23] L. P. Kouwenhoven, D. G. Austing, and S. Tarucha, Rep. Prog. Phys. **64**, 701 (2001), and references therein.
[24] U. Fano, Phys. Rev. **124**, 1866 (1961).
[25] K. Kobayashi, H. Aikawa, S. Katsumoto, and Y. Iye, Phys. Rev. Lett. **88**, 256806 (2002).